J. Chem. Sci. Vol. 127, No. 7, July 2015, pp. 1173–1181.
DOI 10.1007/s12039-015-0878-y

Synthesis and crystal structure determination of $YCo_{1-x}Fe_xO_3$ ($x = 0$, 0.33, 0.5, 0.67 and 1) perovskites

S DIMITROVSKA-LAZOVA[a,*], S ALEKSOVSKA[a,b,c] and P TZVETKOV[d]
[a]University "St. Cyril and Methodius", Faculty of Natural Sciences and Mathematics, Institute of Chemistry, Arhimedova 3, 1000 Skopje, R Macedonia
[b]Research Center for Environment and Materials, Macedonian Academy of Sciences and Arts, Krste Misirkov 2, 1000 Skopje, R Macedonia
[c]Faculty of Medical Sciences, Goce Delcev University, Stip, R Macedonia
[d]Institute of General and Inorganic Chemistry, Bulgarian Academy of Science, "Acad. Georgi Bonchev" bl. 11, 1113 Sofia, Bulgaria
e-mail: sandra@pmf.ukim.mk

MS received 12 November 2014; revised 4 March 2015; accepted 6 March 2015

Abstract. The results on synthesis, crystal structure determination and calculation of crystallochemical parameters of $YCo_{1-x}Fe_xO_3$ ($x = 0$, 0.33, 0.5, 0.67 and 1) perovskites are presented in this work. The compounds within this series were synthesized by solution combustion method using two different fuels: urea and citric acid. It was found that iron-containing perovskites, obtained by citric acid as a fuel are of better quality and crystallinity. All the compounds crystallize in *Pnma* space group with $Z = 4$. According to the structure and the calculated crystallochemical parameters, the coordination number of Y^{3+} in these perovskites is 8. The unit cell parameter relationship is of $O-$type suggesting that the main reason for distortion of ideal perovskite structure is the octahedral tilting. The deformation of the octahedrons, as well as the tilting angles, are increasing with the increasing content of Fe^{3+} but the calculated global instability indices (*GII*) show that the stability of the perovskite structure is increasing with increasing of the Fe^{3+} content.

Keywords. Complex perovskites; XRD; crystal structure; crystallochemical calculations.

1. Introduction

The perovskite type structure is one of the most important structural classes among materials due to their important and specific physical and chemical properties. Thus, depending on the composition and structure, the perovskites could exhibit ferroelectricity, piezoelectricity, conducting property ranging from insulators to superconductivity, colossal magnetoresistance, giant magnetoresistance, etc. Their high thermal stability makes them appropriate also for use as catalyst in a number of catalytic processes.[1–3]

The ideal structure of perovskites (ABX_3) is cubic ($Pm\bar{3}m$) consisting of three-dimensional network of regular corner-linked BX_6 octahedra, the B cations being at the centres of these octahedra and the A cations are located at the centre of the dodecahedral cavities.[4] Despite the simplicity of the original perovskite crystal structure, this family of compounds shows an enormous variety of structural modifications and variants. Thus, the perovskite structure could adopt different A and B cations and anions, but typically A corresponds to lanthanides, actinides, alkaline or alkaline earth metals; B generally corresponds to transition metals and X in most cases is oxygen. Furthermore, in a so-called complex or double perovskites, the A and B-positions could be occupied with two or more different cations. Depending on the types of the ions in the perovskite structure, many different types of distortions can occur from the ideal structure. These include tilting of the octahedra, displacement of the cations from the centres of coordination polyhedra, and Jahn-Teller distortion of the octahedra. In most cases, the physical properties of perovskites that are important for their applications strongly depend on the composition and the details of these distortions.

In recent years, there is a growing interest of rare earth cobaltites partially substituted with other transition metals in B-position. This is mainly due to their interesting electronic and magnetic properties, which results in the possibility of spin-state changes of Co^{3+} ions.[5–8] Thus, it was found that Co^{3+} ion could undergo temperature driven spin-state changes from low-spin (t_{2g}^6) to intermediate-spin ($t_{2g}^5 e_g^1$) and finally to high-spin

*For correspondence

state ($t_{2g}^4 e_g^2$), or it could exist in mixed spin state.[5,9] It should also be pointed out that the obtained structural phase and particle size of perovskites depend on their synthesis, so numerous pathways towards new structures have been developed.

Taking these findings into consideration, and continuing our work on complex perovskites,[10–12] in this study, different synthetic routes and detailed structural investigation of new complex perovskites of general formula $YCo_{1-x}Fe_xO_3$ ($x = 0$, 0.33, 0.5, 0.67 and 1) are presented. Our interest was focused on these perovskites mainly as a result of interesting properties of the well-known simple perovskites, $YCoO_3$ and $YFeO_3$. Namely, $YFeO_3$ was widely studied for its magnetic and magneto-optical properties and the possibility for use in catalysis, in gas sensors and monitoring applications.[13] Also, doped $YCoO_3$ have attracted great attention over the last several decades due to their potentially technological applications in many fields such as thermoelectricity,[14,15] oxygen-permeable ceramic membranes (OPCMs),[16] oxygen electrode catalysts in aqueous alkaline solution batteries,[17] gas sensors,[18] cathode for solid oxide fuel cells (SOFCs),[19] etc.

According to the literature data, the end members of the studied series, $YCoO_3$ and $YFeO_3$, may be synthesized using different methods. The most frequently used method for synthesis of cobalt-containing perovskite is solid state synthesis[20–24] often performed in oxygen atmosphere or under higher pressures.[21–23] Another method used for the preparation of $YCoO_3$ is the sol-gel method.[25] Unlike $YCoO_3$, it is very hard to obtain $YFeO_3$ by conventional solid-state methods of synthesis. Namely, the study of the phase diagram of Y_2O_3-Fe_2O_3 system showed that the formation of compound with garnet structure, $Y_3Fe_5O_{12}$ (Y-Fe garnet) is more favourable.[26] As a consequence, a number of soft-chemistry methods were used to obtain the perovskite phase. For example, $YFeO_3$ was synthesized using sol-gel method,[26–29] solution combustion method with glycine, sucrose or citric acid as fuels,[30,31] via complex precursors,[13] coprecipitation[32] or microwave heating.[33] This perovskite may also be obtained as monocrystal.[34,35] It should be emphasized that crystal structure of $YFeO_3$ heavily depends on the method of synthesis and sintering. For example, hexagonal $YFeO_3$ may be obtained by decomposition of complex precursors followed by heat treatment at low temperature.[13] Hexagonal phase was also obtained using the solution combustion method with glycine or citric acid as fuels.[30,31] Detailed investigations on the solution combustion synthesis using glycine as a fuel pointed out that mainly two factors influence the structure of $YFeO_3$. First factor is the ratio between the glycine and the nitrate ions. The lower ratio ($\sim$1.3) leads to formation of perovskite with hexagonal structure while higher ratio ($>$1.5) to orthorhombic structure.[30] The second factor is the temperature of combustion. It was found that if the combustion is performed at lower temperatures or if lower temperatures of additional heating are applied, the compound with hexagonal structure may be obtained.[31]

In order to investigate the influence of the fuel on the solution combustion synthesis of $YCo_{1-x}Fe_xO_3$ ($x = 0$, 0.33, 0.5, 0.67 and 1) perovskites, in this study solution combustion method was applied using urea or citric acid as fuels. Also, detailed crystal structure determination of the new complex perovskites and the calculated crystallochemical parameters are discussed below.

2. Experimental

For synthesis of $YCo_{1-x}Fe_xO_3$ ($x = 0$, 0.33, 0.5, 0.67 and 1) by solution combustion method, two different fuels were used: citric acid or urea. The starting solutions in all synthesis were prepared by dissolving metal nitrates ($Y(NO_3)_3{\cdot}6H_2O$, $Co(NO_3)_2{\cdot}6H_2O$ and $Fe(NO_3)_3{\cdot}9H_2O$) in a small amount of water. The quantity of the fuel was calculated using the oxidizer/fuel ratio and in all syntheses it was set to 1.

When urea was used as a fuel, it was dissolved in diluted nitric acid (1:1), the solution was slowly added to the water solution of metal nitrates and then slowly heated in a muffle furnace up to $\sim$500°C. After the evaporation of the water the fuel initiated and a self propagated combustion reaction took place resulting in formation of spongy powders.

In the case when citric acid was used as a fuel, the citric acid was dissolved in small quantity of water and was slowly added to the solution containing metal nitrates. According to some literature data[36] regarding the solution combustion synthesis of similar compounds, the synthesis is more successful if the pH of the initial solution is 7 or above. In order to perform the synthesis in neutral solution, the pH of the initial reaction mixture was adjusted with addition of NH_4OH. The as-prepared solutions were heated on magnetic stirrer at temperature of 80°C. After the evaporation of the water (almost completely) the container was transferred on a hot plate preheated at $\sim$300°C, and vigorous combustion reaction started evolving large amount of gases.

The obtained powders, both with urea or citric acid as a fuel, were additionally heated for 4 h at 800°C, yielding perovskites. However, since all synthesized complex perovskites using citric acid contained small

amount of Y_2O_3, they were washed with diluted HCl ($c = 1$ mol/dm^3). After washing and filtration, the samples were dried and additionally heated for 6 h at 950°C.

The crystallinity, purity and crystal structure of the obtained perovskites were studied by powder X-ray diffraction. The diffractograms were recorded on Bruker D8 Advance with $Cu_{K\alpha}$ radiation and SOL-X detector within the range $10-120°2\theta$ at room temperature with step-scanning of 0.02°. The refinements of the crystal structures were performed using the Rietveld method and program package FullProf.[37] Several profile parameters such as background, scale factor, zero shift, two asymmetry parameters and for some samples ($YCo_{0,67}Fe_{0,33}O_3$ and $YCo_{0,5}Fe_{0,5}O_3$) the preferred orientation, were included during the crystal structure refinement.

3. Results and Discussion

3.1 *Synthesis*

As previously stated, in this study $YCo_{1-x}Fe_xO_3$ ($x = 0, 0.33, 0.5, 0.67$ and 1) perovskites were obtained using two different fuels. In both cases, perovskites with same structure were obtained but the purity and the degree of crystallinity was different, so the influence of the fuel on the synthesis of these perovskite materials is obvious.

The XRD patterns (figure 1a) of the iron containing perovskites obtained with urea as a fuel clearly show that these perovskites were not well crystalline and contained impurities mainly from Y_2O_3 (For clarity, only the XRD patterns of $YCo_{0.5}Fe_{0.5}O_3$ are presented). The additional heat treatment (6 h at 900°C and 7 h at 1000°C) did not improve their characteristics (figure 1b). On the other hand, $YCoO_3$ obtained by the same synthetic route (urea as a fuel) was of satisfactory purity and crystallinity (figure 2a). However, further heating (6 h at 800°C; 6 h at 900°C and 5 h at 1000°C) of this perovskite was performed in order to obtain sample suitable for crystal structure refinement.

The XRD-patterns of the perovskites synthesized using citric acid as a fuel, showed that this fuel would be preferable choice in synthesis of iron containing members of this series ($YCo_{1-x}Fe_xO_3$, $x = 0.33$; 0.5; 0.67 and 1). Namely, the purity and the crystallinity of perovskites obtained using citric acid are better in comparison when using urea. It is important to notice that $YCoO_3$ was not obtained when citric acid was used as a fuel (figure 2b). Namely, after the heat treatment at 800°C only mixture of oxides (Y_2O_3 and Co_3O_4) was obtained (figure 2b).

In aim to study the process of forming complex (Co/Fe) perovskites and $YFeO_3$, the XRD patterns of all stages of the combustion synthesis by citric acid were recorded, but for better clarity, only the patterns of $YCo_{0.67}Fe_{0.33}O_3$ are presented (figure 3). After heating of the amorphous precursor samples for 4 h at 800°C, a mixture of perovskite phase and small amount of Y_2O_3 (Y_2O_3, ICDD card #41−1105) was obtained for all samples except for $YFeO_3$, which was obtained as a pure (figure 3a). The impurities of Y_2O_3 were eliminated by washing the samples with diluted HCl and drying afterwards. The XRD patterns of dried samples (figure 3b) showed that the impurities were successfully eliminated. However, in order to obtain powders with better crystallinity, the samples were heated again for 6 h at 950°C, and such obtained perovskites were further used in structural investigations (figure 3c).

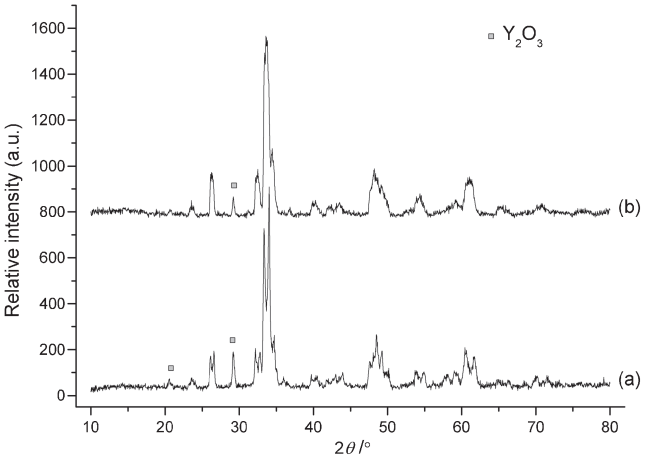

Figure 1. XRD pattern of $YCo_{0.5}Fe_{0.5}O_3$ obtained using urea: (**a**) heated for 4 h at 800°C; (**b**) additionally heated for 7 h at 1000°C.

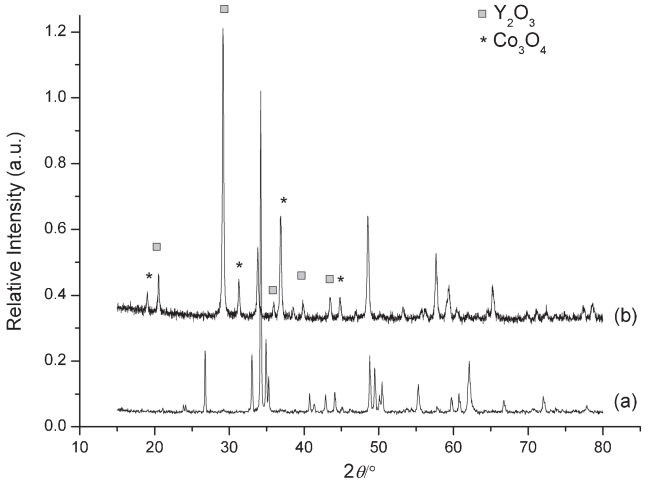

Figure 2. XRD pattern after final heating of $YCoO_3$ synthesized (**a**) using urea and; (**b**) using citric acid as a fuel.

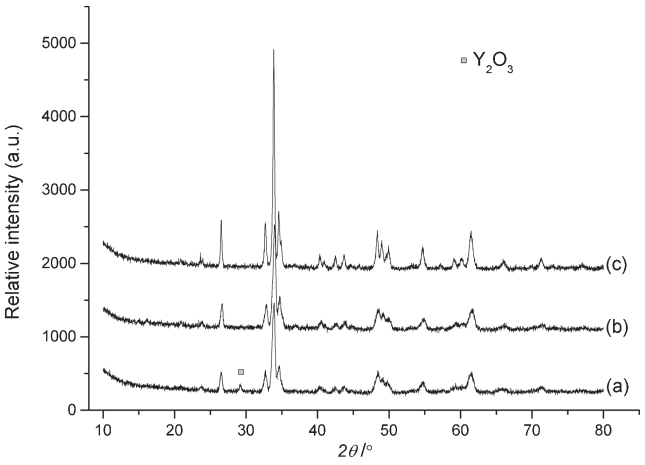

Figure 3. XRD patterns of $YCo_{0.67}Fe_{0.33}O_3$ after (**a**) initial heating (at 800°C for 4 h); (**b**) treatment with HCl (**c**) heating 6 h at 950°C.

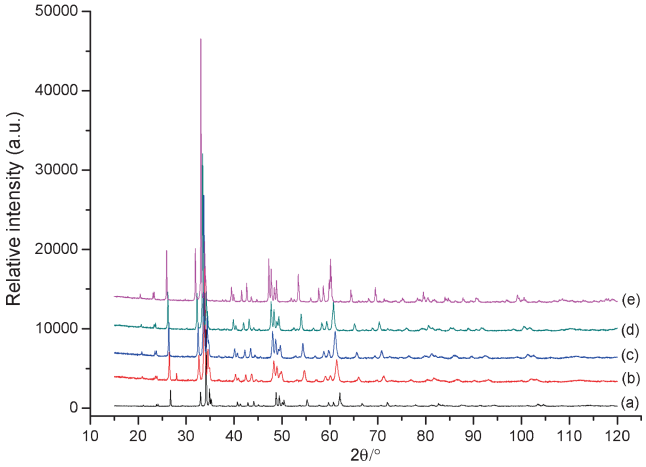

Figure 4. The XRD patterns of perovskites from $YCo_{1-x}Fe_xO_3$ series: (**a**) $YCoO_3$; (**b**) $YCo_{0.67}Fe_{0.33}O_3$; (**c**) $YCo_{0.5}Fe_{0.5}O_3$; (**d**) $YCo_{0.33}Fe_{0.67}O_3$; and (**e**) $YFeO_3$.

The results of the synthesis of $YCo_{1-x}Fe_xO_3$ perovskite series, clearly show that the influence of the fuel is mainly connected with the type of the B-cation. Although both Fe^{3+} and Co^{3+} are hard acids and O^{2-} is considered as a hard base the affinity of Fe^{3+} towards citric acid is very strong. This is probably due to, not just the formation of monoiron dicitrate, but also of formation of binuclear and trinuclear oligomeric complexes.[38]

3.2 *Crystal structure*

The crystal structures of $YCoO_3$ and $YFeO_3$ (end members of the series) have already been refined[24,34] but they are included in this analysis in order to track the structural changes arisen with mutual substitution of Fe and Co. According to the literature data[24] $YCoO_3$ is of orthorhombic structure, space group *Pnma* ($Z = 4$). The other end member of the series, $YFeO_3$, could be hexagonal[30,31] or orthorhombic.[27,31,34,35] Unlike the metastable hexagonal phase, the orthorhombic phase (isomorphous with the other members of $LnFeO_3$ series which are of $GdFeO_3$ structural type), is thermodynamically stable. Also, the study of crystal structure on monocrystal samples revealed orthorhombic structure.[34,35] As it was previously mentioned, there is no literature data about the crystal structure of the complex perovskites obtained with partial substitution of Co with Fe. Therefore, their structures will be thoroughly discussed here.

The XRD patterns of $YCo_{1-x}Fe_xO_3$ are presented on figure 4. The pure single-phase $YFeO_3$ (figure 4e) was indexed as orthorhombic (ICDD card #39−1489). The analogy of the XRD patterns of other members of the series with that of $YFeO_3$ (figure 4), leads to conclusion that all members of the series are orthorhombic and the refinement of the crystal structure of all compounds was performed within the space group *Pnma*. The accordance between the experimental and calculated structures was verified by the Rietveld plot (figure 5).

The unit cell parameters, fractional atomic coordinates and isotropic temperature factors of $YCo_{1-x}Fe_xO_3$ series are given in table 1. The calculated unit cell parameters (table 1) of the simple perovskites, $YCoO_3$ and $YFeO_3$, are in very good agreement with the literature values ($YCoO_3$: $a = 5.4191(5)$ Å, $b = 7.3658(7)$ Å and $c = 5.1388(5)$ Å,[24] and $YFeO_3$: $a = 5.5877(3)$ Å, $b = 7.5951(4)$ Å and $c = 5.2743(7)$ Å[34]).

The values of the unit cell parameters of the complex $YCo_{1-x}Fe_xO_3$ perovskites ($x = 0.33$, 0.5 and 0.67) are between those of the end members (table 1). It may be noticed that as the content of cobalt decreases the

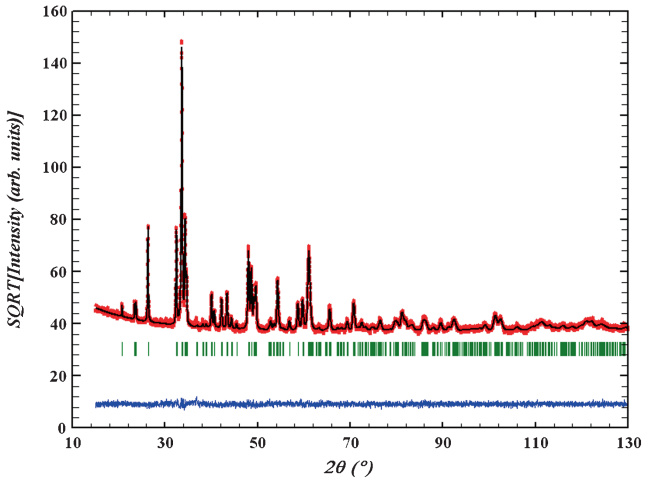

Figure 5. The Rietveld plot of $YCo_{0.5}Fe_{0.5}O_3$.

Table 1. The unit cell parameters, fractional atomic coordinates, isotropic temperature factors and discrepancy factors for $YCo_{1-x}Fe_xO_3$ ($x = 0$, 0.33, 0.5, 0.67 and 1).

		$YCoO_3$	$YCo_{0.67}Fe_{0.33}O_3$	$YCo_{0.5}Fe_{0.5}O_3$	$YCo_{0.33}Fe_{0.67}O_3$	$YFeO_3$
	a/Å	5.42156(7)	5.4770(3)	5.5087(1)	5.53905(18)	5.59245(7)
	b/Å	7.36536(16)	7.4396(3)	7.4807(2)	7.5222(1)	7.60387(10)
	c/Å	5.13809(11)	5.1874(2)	5.2133(1)	5.23740(16)	5.28056(7)
Y	*x*	0.06921(19)	0.06797(16)	0.06816(14)	0.06880(8)	0.06800(10)
	z	0.9819(3)	0.9829(3)	0.9829(2)	0.9826(2)	0.98212(18)
	B	0.35(3)	0.42(3)	0.47(2)	0.33(2)	0.397(20)
Co/Fe	*B*	0.05(4)	0.22(4)	0.19(3)	0.15(4)	0.18(2)
O1	*x*	0.4737(7)	0.4647(11)	0.4663(9)	0.4643(6)	0.4606(7)
	z	0.0952(8)	0.0980(11)	0.0999(9)	0.1037(9)	0.1092(7)
	B	1.5(1)	1.36(19)	1.18(16)	1.18(15)	0.89(11)
O2	*x*	0.3029(11)	0.3034(9)	0.3041(7)	0.3058(7)	0.3062(5)
	y	0.0483(7)	0.0543(5)	0.0539(4)	0.0560(4)	0.0582(3)
	z	0.6947(11)	0.6967(9)	0.6959(6)	0.6951(7)	0.6936(5)
	B	1.30(18)	0.35(16)	0.85(14)	1.04(8)	1.39(10)
R_I	R_p:	5.02	16.7	15.1	14.6	11.8
	R_{wp}:	6.44	11.9	10.9	10.8	9.74
	R_{exp}:	5.59	10.69	9.95	9.95	8.43
	χ^2:	1.32	1.24	1.21	1.19	1.34
	R_B:	4.46	2.98	2.83	2.94	3.07

values of the unit cell parameters increase. This trend is in accordance with the values of ionic radii of B-cations. Namely, in these structures the smaller Co^{3+} ($r(Co^{3+}) = 0.545$ Å, LS) ion is substituted with slightly bigger Fe^{3+} ($r(Fe^{3+}) = 0.645$ Å HS) ion. The relationship between the unit cell parameters in the investigated perovskites is of *O*-type, meaning $a > c$ and $a > b/\sqrt{2} > c$.[4] This relation points out that the main reason for deviation from the ideal perovskite structure is the tilting of the octahedra, which is of $a^+b^-b^-$ type, according to the Glazer's classification.[39]

The values of the unit cell parameters were used to calculate several distortion indices. Thus spontaneous strain (s),[40] which is an indicator for discrepancy of the orthorhombic perovskite from ideal cubic symmetry, was calculated by equation 1

$$s = \frac{2\,(a-c)}{(a+c)} \tag{1}$$

Another distortion index was cell distortion (d)[41] calculated according the equation 2

$$d = \frac{\left[\left(a/\sqrt{2}-a_p\right)^2+\left(b/2-a_p\right)^2+\left(c/\sqrt{2}-a_p\right)^2\right]}{3a_p^2}\times 10^4 \tag{2}$$

where a_p is aristotype cubic lattice parameter calculated by (3)

$$a_p = \frac{\left(a/\sqrt{2}+b/2+c/\sqrt{2}\right)}{3} \tag{3}$$

Finally, an orthorhombic distortion ($dist_{orth}$)[42] was calculated by equation 4

$$dist_{orth} = \frac{\sqrt{\sum (a_i-\bar{a})^2}}{\bar{a}} \tag{4}$$

where, $a_i = a$, c and $b/\sqrt{2}$ and $\bar{a}$ is average from the values of a_i.

It may be noticed (figure 6) that their values are increasing with increasing of the iron content, which means that $YFeO_3$ has the most distorted unit cell in the studied series.

The calculated distances and angles of the perovskites within this series are given in table 2. In table 3

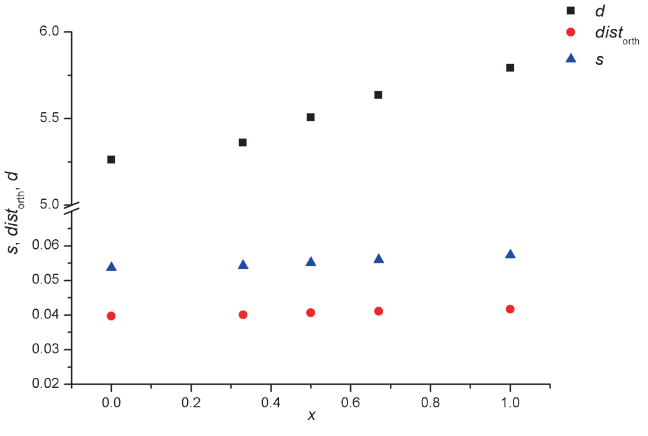

Figure 6. Spontaneous strain (s), cell distortion (d) and orthorhombic distortion of the compounds from $YCo_{1-x}Fe_xO_3$ series.

Table 2. Selected distances (Å) and angles (°) in $YCo_{1-x}Fe_xO_3$ ($x = 0$, 0.33; 0.5; 0.67 and 1) perovskites.

	$x = 0$	$x = 0.33$	$x = 0.5$	$x = 0.67$	$x = 1$
Y−O1	3.281(7)	3.358(5)	3.371(3)	3.408(4)	3.463(3)
	2.269(7)	2.253(5)	2.276(4)	2.281(4)	2.296(3)
	3.010(7)	3.066(5)	3.09(4)	3.125(4)	3.180(3)
	2.234(7)	2.246(5)	2.246(4)	2.243(4)	2.240(3)
(Y−O2) x 2	2.447(5)	2.447(4)	2.466(3)	2.474(3)	2.495(2)
	2.262(5)	2.256(4)	2.266(3)	2.262(3)	2.265(2)
	3.414(5)	3.468(4)	3.490(3)	3.529(3)	3.578(2)
	2.550(4)	2.618(4)	2.626(3)	2.649(3)	2.690(2)
(B−O1) x 2	1.9105(18)	1.9378(16)	1.9502(8)	1.9674(14)	1.9987(7)
(B−O2) x 2	1.956(5)	1.991(4)	2.003(3)	2.023(3)	2.043(2)
	1.931(5)	1.949(4)	1.960(3)	1.971(3)	1.997(2)
<B−O>	1.933	1.959	1.971	1.987	2.012
B−O1−B	149.07(6)	147.40(7)	147.06(5)	145.83(5)	144.02(4)
(B−O2−B) x 2	147.9(1)	146.37(20)	146.27(16)	145.28(15)	144.33(8)

other important crystallographic parameters calculated from the fractional atomic coordinates, are presented. The analysis of some selected distances (table 2) showed that Y−O and Co/Fe−O distances are increasing with increasing of iron content. Unlike in the ideal perovskite structure, the values of Y−O distances within YO_{12} polyhedron are not equal - eight of them being at shorter and four at longer distances and as a consequence the coordination polyhedron around Y^{3+} ion is considerably distorted. This led toward lowering of the coordination number of Y-cations from 12 (crucial characteristic of ideal perovskites) to 8. In order to confirm these findings, the deformation indices Δ_8 and Δ_{12} (table 3) were calculated. The deformation index is used to evaluate the distortion of the coordination polyhedron and is calculated by the equation:[43]

$$\Delta = \frac{1}{n}\sum_i \left[\frac{(r_i - r)}{r}\right]^2 \cdot 10^3 \qquad (5)$$

where, r_i is the particular bond distance; r is the average value of the bond distances and n is the number of bonds in the polyhedron. In regular polyhedrons the value of Δ is close to 0. Taking into account the Δ values of the studied series it may be noticed that the polyhedron around Y is becoming more irregular as the content of iron is increasing. Also, comparing the values of Δ_8 and Δ_{12} it may be noticed that the values of Δ_{12} are considerably higher suggesting that the coordination number of yttrium in this perovskite series is 8. Analyzing the values of the individual Y−O distances it may be noticed (table 2) that the increase of Y−O distance with increasing the iron content is mostly pronounced in the long distances while short Y−O distances are enhancing only slightly with increasing content of Fe^{3+} ion.

Table 3. Distortion indices, Δ, observed tolerance factors, t_o, and global instability index, *GII*, of the $YCo_{1-x}Fe_xO_3$ ($x = 0$, 0.33; 0.5; 0.67 and 1) perovskites.

	Δ_8	Δ_{12}	Δ_6	$t_o(6)$	$t_o(7)$	*GII*
$YCoO_3$	2.835	27.965	0.0927	0.870	0.980	0.2414
$YCo_{0.67}Fe_{0.33}O_3$	4.058	30.529	0.1390	0.864	0.977	0.2360
$YCo_{0.5}Fe_{0.5}O_3$	4.013	30.644	0.1353	0.863	0.977	0.2055
$YCo_{0.33}Fe_{0.67}O_3$	4.529	32.315	0.1694	0.858	0.975	0.1643
$YFeO_3$	5.340	34.045	0.1119	0.853	0.973	0.0720

According to the literature data,[34,35] the mean value of the iron-oxygen distances in $YFeO_3$ is similar to the one in yttrium-iron garnet structures (2.00 Å). The average Fe−O distance in this study is also very close to 2.00 Å (precisely it is 2.012 Å). This fact suggested that the average Fe^{3+}−O^{2-} distance in $YFeO_3$ is independent of the distortion of the perovskite lattice. In complex perovskites, however, the obtained B−O distances are shorter due to mutual substitution of Fe^{3+} with smaller Co^{3+} ions. In average, this results in distortion of the BO_6 octahedrons. The estimation of the octahedral distortion is given by the calculated Δ_6 index (table 3).

The increasing of distortion of MO_6 octahedron is followed by increasing of the tilt angles (figure 7). The values of tilt angles may be calculated on the basis of B−O−B (<Co/Fe−O1,2−Co/Fe>) angles

$$\phi^* = (180^\circ - \langle B - O - O\rangle)/2 \qquad (6)$$

or using the relative atomic coordinates:[4]

$$\tan\theta = \left\{\left[\frac{4\sqrt{\left(u_{O1}^2 + v_{O1}^2\right)}}{b}\right]\right\} \qquad (7)$$

$$\tan\theta = \left\{\left[\frac{4\sqrt{2w_{O2}}}{\sqrt{(a^2+c^2)}}\right]\right\} \tag{8}$$

$$\tan\phi = \left[4\sqrt{\frac{(u_{O2}^2+v_{O2}^2)}{(a^2+c^2)}}\right] \tag{9}$$

$$\cos\,\Phi = \cos\,\theta\,\cos\varphi \tag{10}$$

where u, v and w are the displacement of the atomic coordinates from the positions in the ideal cubic structure.

As it can be seen (figure 7) the tilt angles are increasing with increase of the content of iron in the compound. The increase of the tilting angles of the octahedra is reflected in deviation of B–O1–B and B–O2–B angles from 180°– the value characteristic for the ideal cubic structure. These values are suggesting less overlap of Co/Fe-3*d* orbitals with O-2*p* orbitals. The typical geometry of the particular orthorhombic tilted structure of this series is presented on figure 8.

This trend is also in accordance with the calculated values for the so-called observed tolerance factor, t_o, calculated by the equation given by Sasaki *et al*:[41]

$$t_o = \frac{\langle A-O\rangle}{\sqrt{2}\,\langle B-O\rangle} \tag{11}$$

Namely, the values of t_o, assuming coordination number 8 for Y^{3+} ions (as well as those for coordination number 12), are decreasing with increase of iron content. Linear decrease of these values underlines a systematic increase of the deformation of perovskite structure within the studied series. In general, the octahedra in complex perovskites are deformed and tilted to enable the formation of perovskite structure. In order to estimate the overall stability of perovskite structure

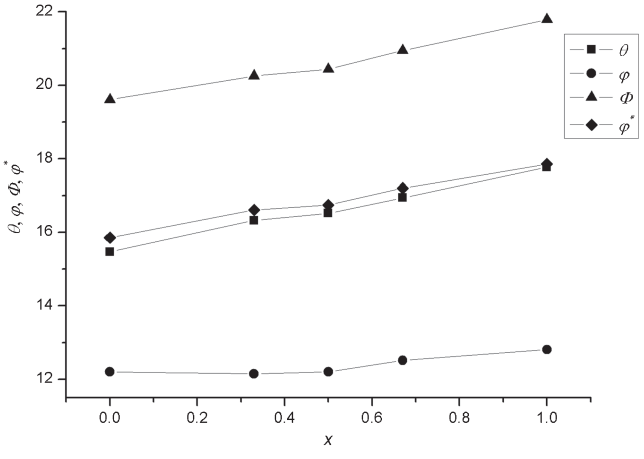

Figure 7. Variation of the values of tilt angles with increasing content of Fe^{3+}.

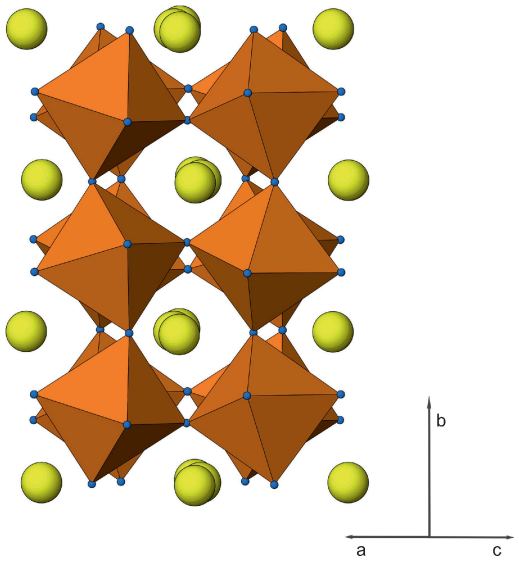

Figure 8. The polyhedron presentation of orthorhombic tilted structure of $YCo_{1-x}Fe_xO_3$.

within the $YCo_{1-x}Fe_xO_3$ series, the Global instability index (*GII*) was calculated,[44] taking into account bond-valence model. According to bond-valence model, the bond valence of the i^{th} ion with respect to the j^{th} ion, s_{ij}, is calculated using equation

$$s_{ij} = \exp\left(\frac{R_{ij}-d_{ij}}{B}\right) \tag{12}$$

where d_{ij} is the cation-anion bond distance; R_{ij} is tabulated value[45] which is empirically determined for each cation-anion pair and is based on a large number of well-determined bond distances for the pair in question and B is an empirically determined universal constant with a value of 0.37. The atomic valences of i^{th} ion $V_{i(calc.)}$ can be calculated as a sum of the individual bond valences (s_{ij}) about each ion:

$$V_{i(calc)} = \sum_j s_{ij} \tag{13}$$

The global instability index (*GII*), could be calculated from the equation

$$GII = \left\{\left[\sum_{i=1}^{N}\left(d_i^2\right)\right]/N\right\}^{1/2} \tag{14}$$

where d_i is the discrepancy between the calculated bond valence and the theoretical oxidation number and N is the number of atoms in the asymmetric unit. The obtained values for *GII* could be an indicator for the presence of strain in the structures that can lead to its

instability. If the structure is of no internal stress, the values of *GII* should be below 0.1 v.u., but in structures with lattice-induced strains, the *GII* values might be 0.2 or above. According to the calculated values for *GII* (table 3), the complex perovskites, as well as $YCoO_3$, are structures with internal stress. The reasons are very subtle, and some authors believe that the main cause is the possibility that a fraction of Co^{3+} ions undergoes spin transition from low-spin to intermediate spin state.[5] As to the complex perovskites, it is evident (table 3) that the value of *GII* decreases with increasing of iron content.

4. Conclusion

The perovskites within the series $YCo_{1-x}Fe_xO_3$ ($x = 0$, 0.33, 0.5, 0.67 and 1) were obtained by solution combustion method using urea or citric acid as a fuel. $YCoO_3$ was not obtained when citric acid was used as a fuel, but was obtained with very good purity and crystallinity by urea synthetic route. Iron-containing perovskites were synthesized by both fuels, but it was found that better morphology of the crystals could be obtained with citric acid. The Rietveld crystal structure determination showed that the perovskites within this series are isomorphous and crystallize in *Pnma* space group with $Z = 4$. On the basis of the relationship between the unit cell parameters in the investigated perovskites, it could be concluded that they are of *O*-type meaning $a > c$ and $a > b/\sqrt{2} > c$, which pointed out that the main reason for deviation from the ideal perovskite structure is tilting of the octahedra. The calculated values for stress, strain, cell distortion and orthorhombic distortion increase with increasing iron content, which means that $YFeO_3$ has the most distorted unit cell in the studied series. According to the obtained distances and angles, the coordination number of Y in these perovskites is 8. The calculated deformations of the octahedra, as well as the tilting angles, showed that they increase with the increasing of Fe^{3+} content. On the contrary, the calculated global instability indices (*GII*) show that the stability of the perovskite structure is increasing with increasing of the Fe^{3+} content. In general, it could be concluded that substitution of Co^{3+} with Fe^{3+} leads to more distorted and tilted octahedron, which is necessary for the formation and stabilization of the perovskite structure.

Acknowledgements

The financial support of the BAS-MANU Collaborative Project "Structural characterization and investigation of electrical and catalytic properties of new synthesized complex perovskites" is gratefully acknowledged.

References

1. Galasso F S 1990 In *Perovskites and High Tc Superconductors* (New York: Gordon and Breach) p. 171
2. Peña M A and Fierro J L G 2001 *Chem. Rev.* **101** 1981
3. Ishihara T (Ed.) 2009 *Perovskite Oxide for Solid Oxide Fuel Cells* (Dordrecht: Springer)
4. Mitchell R H 2002 In *Perovskites: Modern and Ancient* (Thunder Bay: Almaz) p. 9
5. Knížek K, Jirák Z, Hejtmánek J, Veverka M, Maryško M, Maris G and Palstra T T M 2005 *Eur. Phys. J. B* **47** 213
6. Yan J-Q, Zhou J-S and Goodenough J B 2004 *Phys. Rev. B* **69** 134409
7. Cavalcante F H M, Carbonari A W, Malavasi R F L, Cabrera-Pasca G A, Saxena R N and Mestnik-Filho J 2008 *J. Magn. Magn. Mater.* **320** e32
8. Zhou J-S, Yan J-Q and Goodenough J B 2005 *Phys. Rev. B* **71** 220103R
9. Goodenough J B (Ed.) 2001 In *Localized to Itinerant Electronic Transition in Perovskite Oxides* (Berlin: Springer-Verlag) p. 38
10. Dimitrovska-Lazova S, Kovacheva D, Aleksovska S, Marinšek M and Tzvetkov P 2012 *Bulg. Chem. Comm.* **44** 235
11. Kovachev S, Kovacheva D, Aleksovska S, Svab E and Krezhov K 2009 *J. Optoelectron. Adv. Mater.* **11** 1549
12. Dimitrovska-Lazova S, Kovacheva D and Tzvetkov P 2012 *Bulg. Chem. Comm.* **44** 245
13. Gil D M, Navarro M C, Lagarrigue M C, Guimpel J, Carbonio R E and Gómez M I 2011 *J. Therm. Anal. Calorim.* **103** 889
14. Liu Y, Qin X Y, Wang Y F, Xin H X, Zhang J and Li H J 2007 *J. Appl. Phys.* **101** 083709
15. Liu Y, Li H, Li Y and Sun W 2013 *Ceram. Int.* **39** 8189
16. Yin X, Hong L and Liu Z-L 2006 *Appl. Catal. A: General* **300** 75
17. Lal B, Raghunandan M K, Gupta M and Singh R N 2005 *Int. J. Hydrogen Energy* **30** 723
18. Salker A V, Choi N-J, Kwak J-H, Joo B-S and Lee D-D 2005 *Sens. Actuators, B* **106** 461
19. Rossignol C, Ralph J M, Bae J-M and Vaughey J T 2004 *Solid State Ionics* **175**
20. Thornton G, Morrison F C, Partingtont S, Tofield B C and Williams D E 1988 *J. Phys. C: Solid State Phys.* **21** 2871
21. Demazeau G, Pouchard M and Hagenmuller P 1974 *J. Solid State Chem.* **9** 202
22. Knížek K, Jirák Z, Hejtmánek J, Veverka M, Maryško M, Hauback B C and Fjellvåg H 2006 *Phys. Rev. B* **73** 214443
23. Balamurugan S and Takayama-Muromachi E 2006 *J. Solid State Chem.* **179** 2231
24. Mehta A, Berliner R and Smith R W 1997 *J. Solid State Chem.* **130** 192
25. Buassi-Monroy O S, Luhrs C C, Chávez-Chávez A and Michel C R 2004 *Mater. Lett.* **58** 716

26. Mathur S, Veith M, Rapalaviciute R, Shen H, Goya G F, Martins Filho W L and Berquo T S 2004 *Chem. Mater.* **16** 1906
27. Cao X 2001 *J. Am. Ceram. Soc.* **84** 1265
28. Gatelytė A, Jasaitis D, Beganskienė A and Kareiva A 2011 *Mater. Sci.* **17** 302
29. Maiti R, Basu S and Chakravorty D 2009 *J. Mag. Mag. Mater.* **321** 3274
30. Wu L, Yu J C, Zhang L, Wang X and Li S 2004 *J. Solid State Chem.* **177** 3666
31. Hui S, Jiayue X and Anhua W 2010 *J. Rare Earths* **28** 416
32. Tien N A, Almjasheva O V, Mittova I Ya, Stognei O V and Soldatenko S A 2009 *Inorg. Mater.* **45** 1304
33. Liu J, Xie J M, Zhang H, Gu Z J and Meng X 2007 *Mater. Sci. Forum* **561–565** 1085
34. Du Boulay D, Maslen E N, Streltsov V M and Ishizawa N 1995 *Acta Crystallogr.* **B51** 921
35. Coppens P and Eibschütz M 1965 *Acta Crystallogr.* **19** 524
36. Deganello F, Marcì G and Deganello G 2009 *J. Eur. Ceram. Soc.* **29** 439
37. Rodriguez-Carvajal J 1993 *Physica B* **192** 55
38. Silva A M, Kong X, Parkin M C, Cammack R and Hider R C 2009 *Dalton Trans.* **40** 8616
39. Glazer A M 1972 *Acta Crystallogr.* **B28** 3384
40. Alonso J A, Martínez-Lope M J, de la Calle C and Pomjakushin V 2006 *J. Mater. Chem.* **16** 1555
41. Sasaki S, Prewitt C and Liebermann R 1983 *Am. Mineral.* **68** 1189
42. Huo G, Song D, Yang Q and Dong F 2008 *Ceram. Int.* **34** 497
43. Shannon R D 1976 *Acta Crystall.* **A32** 751
44. Salinas-Sanchez A, Garcia-Munoz J L, Rodriguez-Carvajal J, Saez-Puche R and Martinez J L 1992 *J. Solid State Chem.* **100** 201
45. Brown I D 2009 *Chem. Rev.* **109** 6858